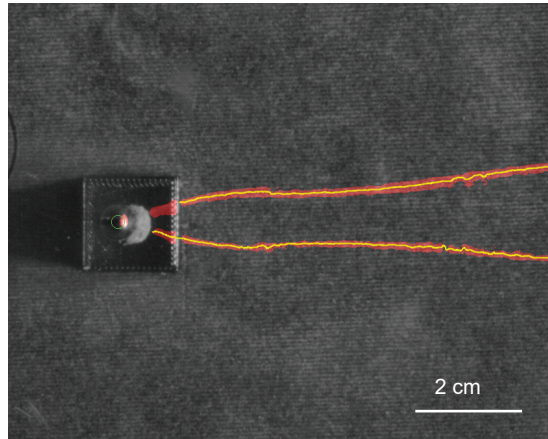


A



B

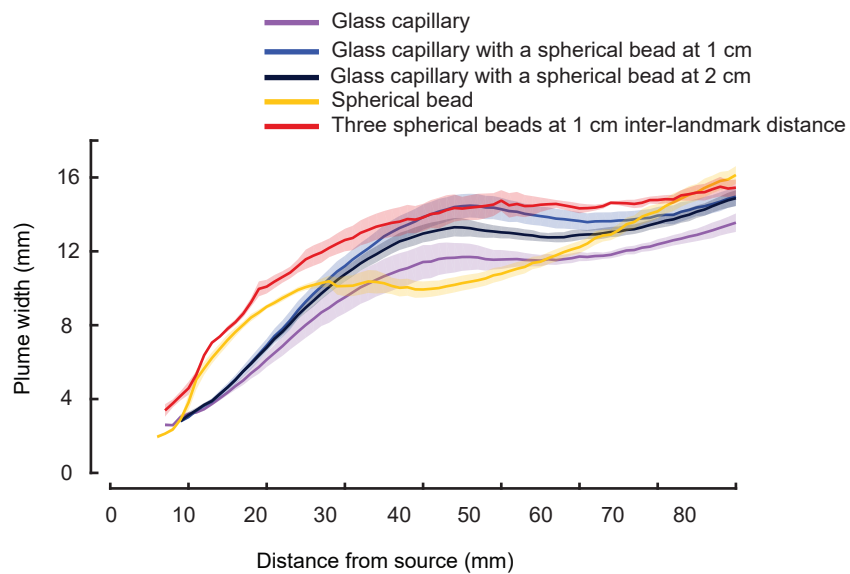
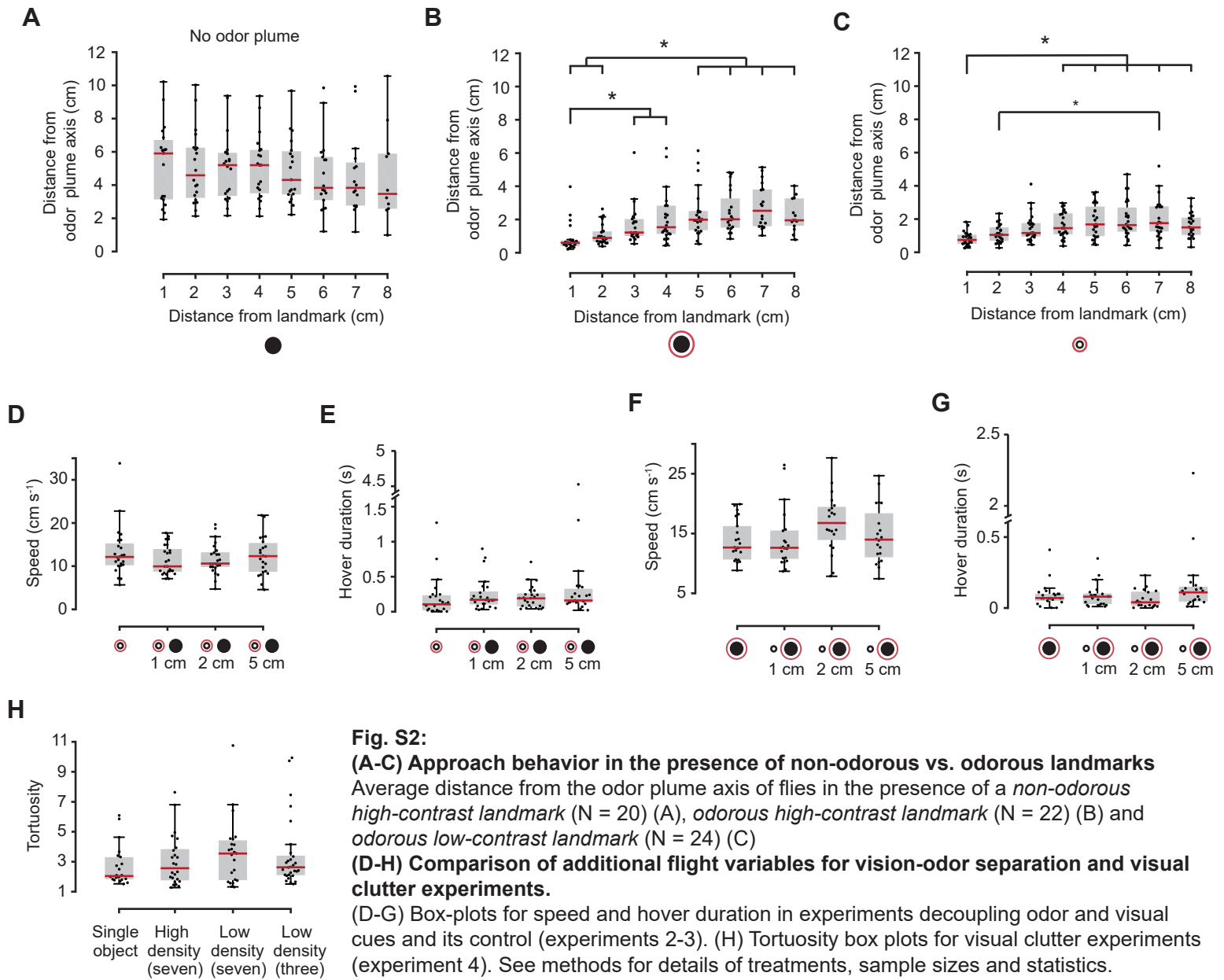


Fig. S1: Plume visualization and quantification of plume width. (A) Steady state smoke plume, viewed from above for a spherical bead (*high-contrast landmark*, $N = 4$). (B) Variation in plume width vs. distance from the source along the plume axis for smoke-visualized plumes. Colors represent specific treatments. Dark lines show the mean plume width and the light bands show the standard error around mean.



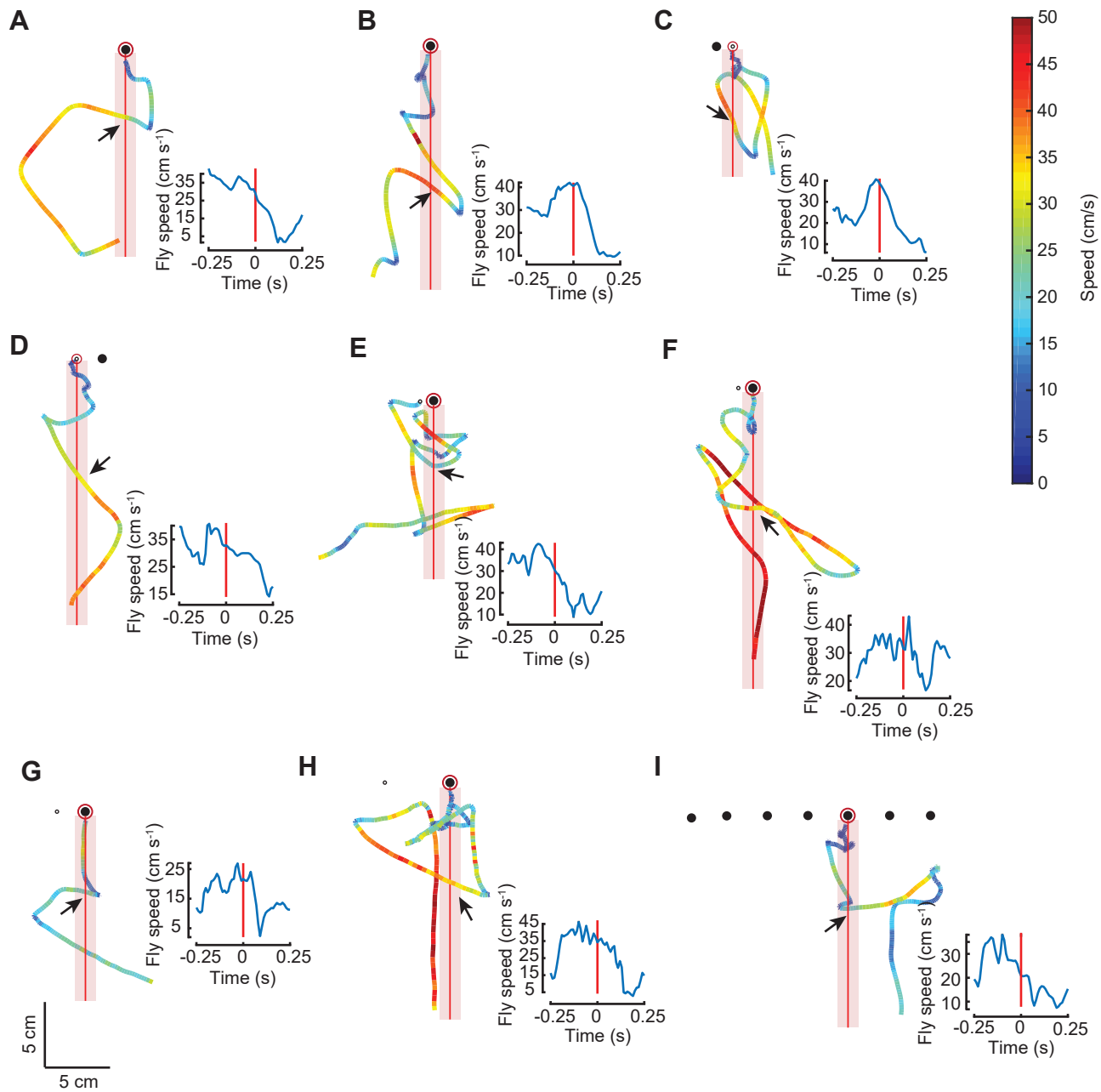


Fig. S3: Examples of trajectory plots that show how speed changes in flies after odor encounter. Sample trajectories of flies in different landmark arrangements show how flies decelerate following odor encounters (arrows). Their speed as a function of time in the 500 ms window around the odor encounter (red vertical bar) is shown in the inset plots. Plume axis (red line) is enveloped by the cylindrical odor plume, estimated to be approximately 1.6 cm wide (light red band). Color map depicts the flight speed.

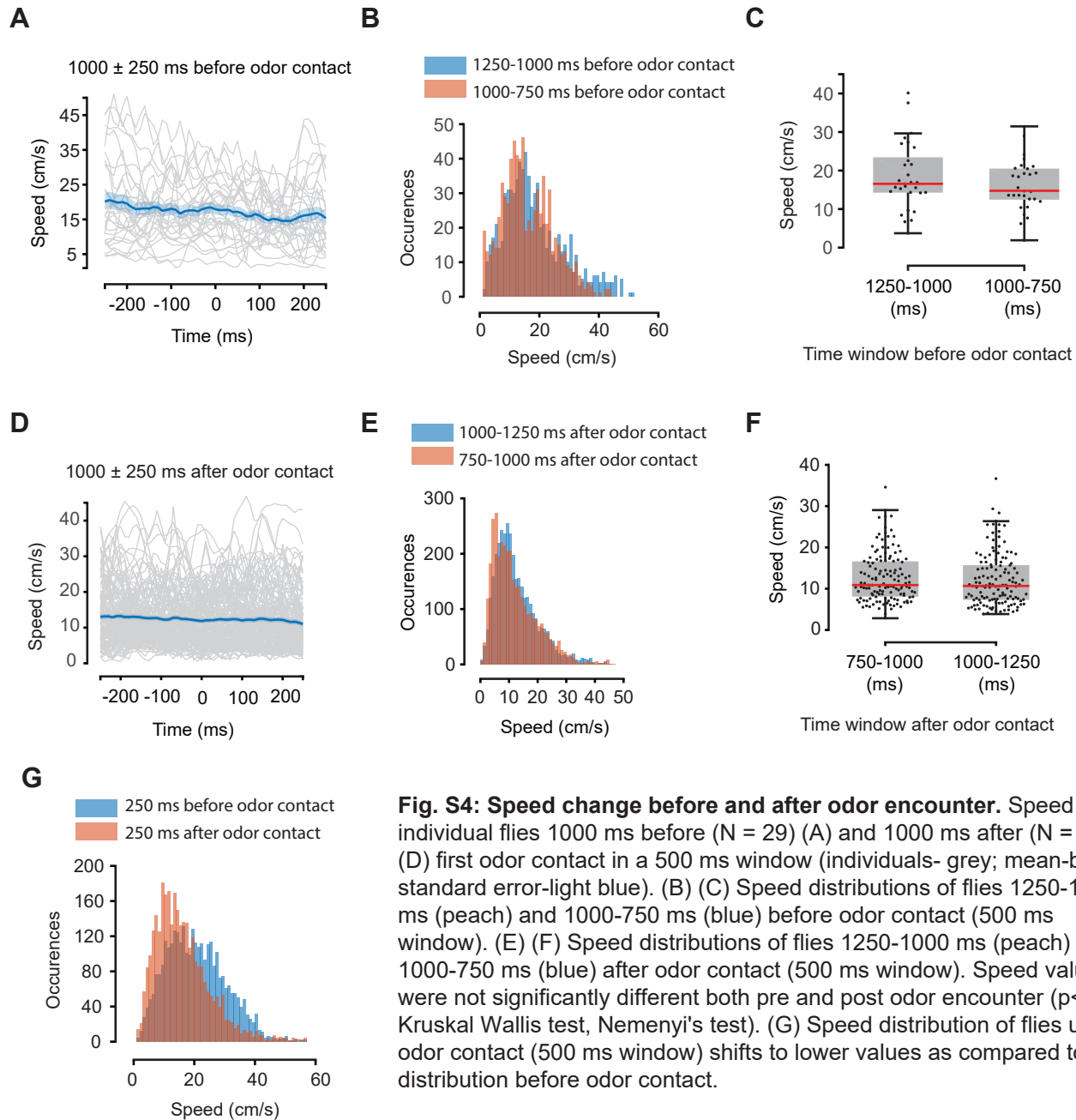


Fig. S4: Speed change before and after odor encounter. Speed of individual flies 1000 ms before ($N = 29$) (A) and 1000 ms after ($N = 134$) (D) first odor contact in a 500 ms window (individuals- grey; mean-blue; standard error-light blue). (B) (C) Speed distributions of flies 1250-1000 ms (peach) and 1000-750 ms (blue) before odor contact (500 ms window). (E) (F) Speed distributions of flies 1250-1000 ms (peach) and 1000-750 ms (blue) after odor contact (500 ms window). Speed values were not significantly different both pre and post odor encounter ($p < 0.05$, Kruskal Wallis test, Nemenyi's test). (G) Speed distribution of flies upon odor contact (500 ms window) shifts to lower values as compared to their distribution before odor contact.

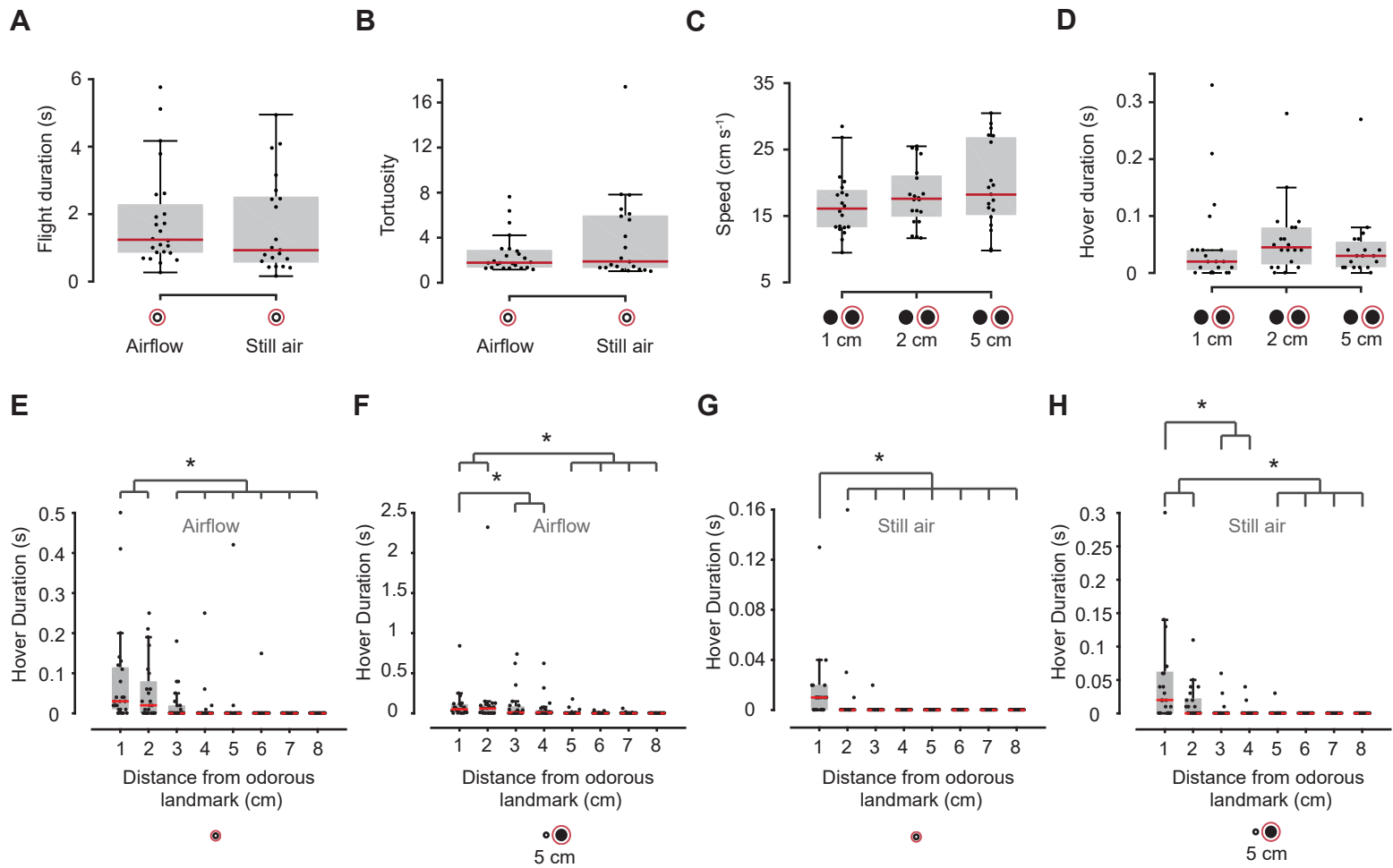


Fig. S5:

(A-D) Comparison of additional flight variables still air experiments.

Flight duration (A) and tortuosity (B) of the flies tracking a low-contrast odorous landmark in the presence or absence of airflow. Speed (C) and hover duration (D) of flies tracking a high-contrast odorous landmark in the presence of a high-contrast non-odorous landmark at 1, 2 and 5 cm.

(E-H) Hover duration increases prior to landing in the presence and absence of airflow.

Comparison of hover duration for the two identical treatments in the presence (E-F) and absence (G-H) of airflow. Asterisks indicate significant differences ($p < 0.05$, Kruskal Wallis test, Nemenyi's test; see Methods for details).

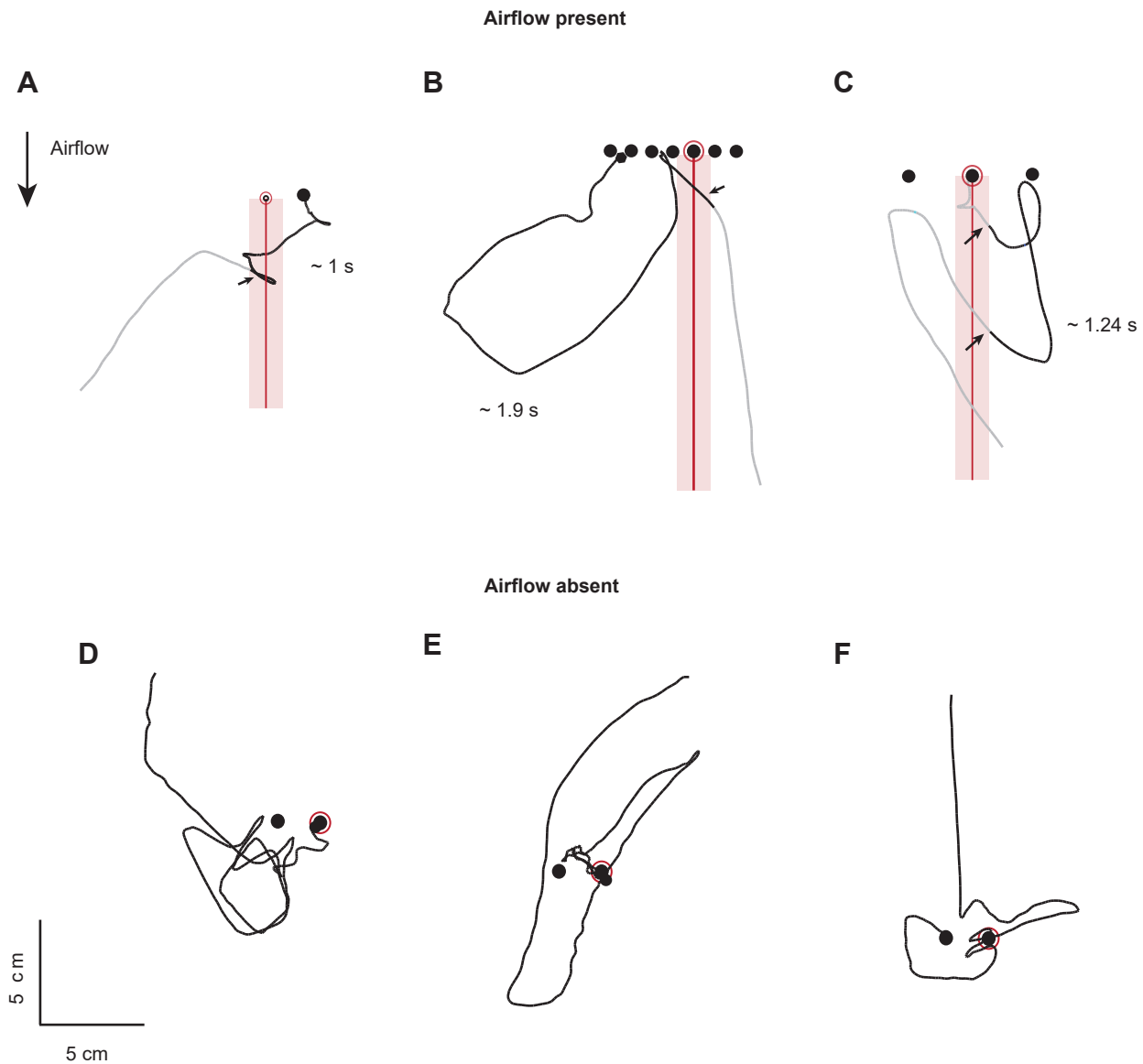


Fig. S6: Sample flight trajectories of flies searching for odor source in presence (A-C) and absence (D-F) of airflow.

(A-C) Trajectories of flies that search for an odor source after exiting the odor plume for (A) ~1 sec, (B) ~1.9 sec, and (C) ~1.24 sec. The segments of flight trajectories in which flies were outside the odor plume after odor contact are highlighted in black and the rest of the trajectory is shown in gray color.

(D-F) Sample trajectories illustrating search for the odorous landmark in absence of airflow.



Movie 1. Smoke plume visualization for various configurations of glass capillary (low-contrast landmark) and spherical bead (high-contrast landmark) objects. These tests ascertain the laminarity of the flow for the different conditions, and also help determine the average width of the odor plume when the airflow in the wind tunnel is set at 0.1 m/s (see Fig. 1B,C and Fig. S1). Diameter of the bead is 6 mm and glass capillary is 1 mm. Smoke was generated using incense